*Subcontractor Report*

# Alternative Heterojunction Partners for CIS-Based Solar Cells

## Final Report
## 1 January 1998–31 August 2001

L.C. Olsen
*Washington State University at Tri-Cities*
*Richland, Washington*

**NREL**

**National Renewable Energy Laboratory**

January 2003   •   NREL/SR-520-33362

# Alternative Heterojunction Partners for CIS-Based Solar Cells

## Final Report
## 1 January 1998–31 August 2001

L.C. Olsen
*Washington State University at Tri-Cities*
*Richland, Washington*

NREL Technical Monitor:  B. von Roedern

**NREL**

**National Renewable Energy Laboratory**

**NOTICE**

# TABLE OF CONTENTS

# LIST OF FIGURES

# LIST OF TABLES

# ABSTRACT

This report summaries work carried out in three areas, CIGSS cells based on ZnO buffer layers, cells with ZnS buffer layers and general studies of the effects of buffer layers on device performance. These investigations were conducted mainly with CIGSS substrates provided by Siemens Solar Industries. ZnO buffer layers were grown by MOCVD and ZnS layers were deposited by chemical bath deposition. Active area efficiencies of 13.4 % and 12.8% were achieved for cells based on ZnO and ZnS buffer layers, respectively. The initial step in the WSU cell fabrication process involves cleaning of the CIGSS surface followed by an etching step with KCN. Studies were carried out to characterize the effect of the KCN step. Using XPS surface analyses as well as XPS depth concentration profiles, it was determined that the KCN etching process removes oxygen that had reacted with the CIGSS surface to form $SeO_2$. Removal of oxygen from the CIGSS surface allows one to fabricate efficient CIGSS cells. Spectroscopic ellipsometry was utilized to determine that a two step MOCVD growth process leads to ZnO layers with a well defined electron band structure whereas a simpler one step process results in more amorphous-like films. In an effort to understand the positive effects of buffer layers in CIS solar cells, I-V analyses have been combined with modeling studies using PC-1D. Although buffer layers may provide passivation at the surface, and possibly inversion in some cases, we conclude that it is also likely that buffer layers provide barriers to impurity diffusion resulting from deposition of TCO layers.

# 1. INTRODUCTION

## 1.1 Background

Previous studies primarily involved investigations of cells based on CIS and CIS alloys with with highly resistive ZnO buffer layers grown by MOCVD. Cells were fabricated by utilizing CIGS substrates from provided by NREL, and CIS and CIGSS substrates from Siemens Solar. One cell based on NREL CIGS and a MOCVD ZnO buffer layer exhibited an active area efficiency of nearly 14 %. Glancing incidence XRD studies conducted at NREL established that the MOCVD buffer layers were truly ZnO, and not an alloy resulting from interdiffusion of ZnO and CIGS. It also was determined that best cells are obtained by using a two step growth process involving growth of ZnO at 100 °C after first heat -treating the CIS-alloy substrate at 250 C. In order to achieve high efficiencies, it was also determined that the buffer layer resistivity needs to be greater than $10^4$ ohm-cm. A limited effort was also devoted to investigations of ZnSe buffer layers.

## 1.2 Program Objectives And Technical Approach

The primary objective of this program was to investigate approaches to fabricating efficient thin-film solar cells based on CIS or a related alloy, and a non-cadmium heterojunction partner. Cells have been investigated with structurtes as described in Figure 1. The term CIS substrate refers to a p-type, polycrystalline CIS layer grown onto Mo-coated glass. Efforts concentrated on utilizing MOCVD-deposited ZnO buffer layers to fabricate state of the art $Cu(In,Ga)Se_2$ solar cells. Studies of chemically deposited ZnS as an alternative heterojunction partner were also carried out. Finally, current-voltage analyses combined with simulation studies using PC-1D were conducted in an effort to deevelop more understanding of the role of buffer layers in CIS-based solar cells.
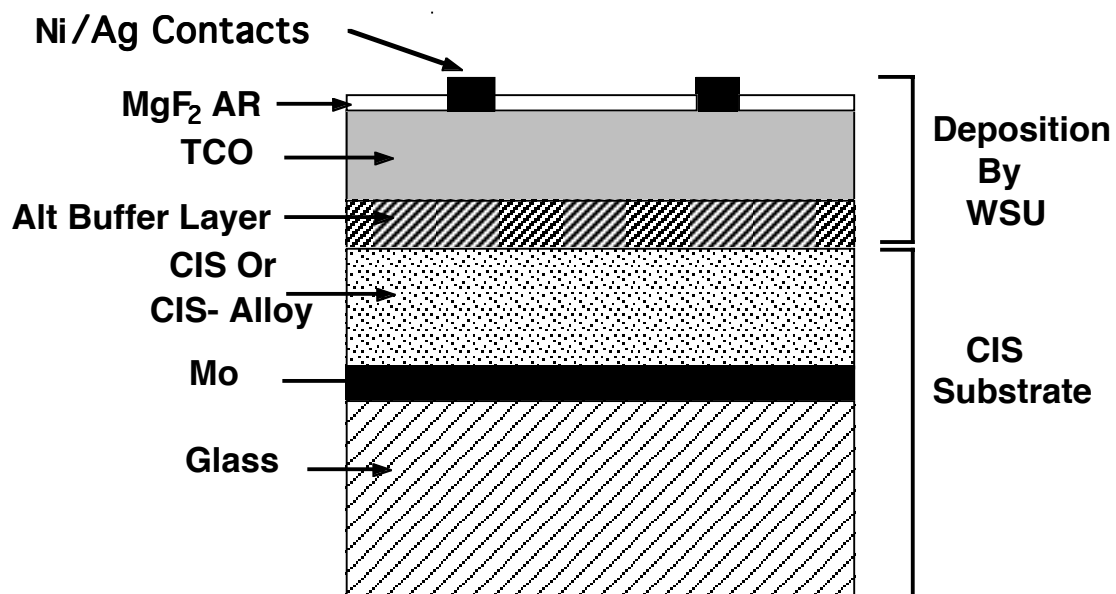
**Figure 1.** Basic solar cell structure investigated in this program. The alternative heterojunction partner is assumed to be slightly n-type, and highly resistive.

## 2. HIGH EFFICIENCY CIS CELLS WITH MOCVD ZnO BUFFER LAYERS

The WSU group has worked with other members of the TFPP program to investigate CIS-alloy cells with MOCVD ZnO buffer layers. Properties of some of the best cells are tabulated in Table 1. Efficiencies over 12 % have now been obtained with the WSU buffer layers for three different types of material, namely, SSI CIS (no longer produced), SSI CIGSS and NREL CIGS. The result for CIGSS was achieved within the last year, while the results for SSI CIS and NREL material were obtained a few years ago. The buffer layers for the CIS and NREL substrates were grown with a two step process involving growth of 100 Å at 250°C followed by growth of 600 Å at 100°C. Furthermore, hydrogen was used as a carrier gas for these studies. During the past two years, we have concentrated on developing a growth process appropriate for the SSI CIGSS material. It was determined that a different procedure than used with the other material was necessary. Very little effort has been devoted to use of NREL material. A key objective of the proposed program is to concentrate more effort towards collaboration with NREL to investigate the use of MOCVD ZnO buffer layers with their CIGS absorbers. As noted above, a different process was utilized for the SSI CIGSS material than with the SSI CIS absorber. In general, we expect that an optimum process for one absorber may not be appropriate for another. Studies carried out to determine an appropriate process for SSI CIGSS material are discussed in the next section.

### 2.1 Process Development For CIGSS Material

Much of the WSU effort to develop ZnO buffer layers has been carried out with SSI CIS and CIGSS substrates. We were provided with 10 cm x 10 cm

**Table 1 --  CIS-Based Cells With MOCVD ZnO Buffer Layers**

| Substrate | Jsc (mA/cm$^2$) | Voc (Volts) | FF ( % ) | Efficiency ( % ) |
|---|---|---|---|---|
| NREL CIGS (Active Area) | 34.5 | 0.581 | 69.2 | 13.9 |
| SSI CIS (Total Area) | 40.7 | 0.439 | 66.9 | 12.0 |
| SSI CIGSS | 33.08 | 0.577 | 66.55 | 12.7 |

absorber plates consisting a CIS or CIGSS layer deposited on a Mo-coated glass substrate.   Cell studies were carried out with 2 cm x 2 cm substrates diced from the 10 cm x 10 cm plates.   Cell processing typically involves surface preparation, buffer layer growth, TCO deposition followed by collector grid and AR coating deposition.   Surface preparation originally involved only a cleaning process consisting of rinses in 1,1,1-trichlorethane, acetone, methanol and distilled water. However, it was eventually determined that etching of the substrate surface with a 10 % KCN solution resulted in superior cell performance.   The effects of the KCN etchant are discussed below.

As noted above, work with SSI CIS and NREL CIGS substrates involved the use of a two step process with hydrogen as a carrier gas.  It was determined that a modified procedure gave better results for the SSI CIGSS material.  Instead of hydrogen, nitrogen was used as a carrier gas and although the sample was heated to 250°C, no film growth occurred until the sample was cooled to 100°C. An additional modification of our growth procedure involved adding water to the THF precursor. The growth process is described by Figure 2.  This process consistently yields very resistive i-ZnO films (>1E4 ohm-cm).        After growth of i-ZnO buffer layers, cells were completed by depositing n-ZnO TCO layers followed by deposition of Ni/Ag or Ni/Al collector grids.  TCOs were deposited by RF sputtering at the Institute of Energy Conversion (IEC) or by CVD at Siemens Solar Industries (SSI).   This process has resulted in cells with total area

efficiencies greater than 11 %. Figure 3 gives current-voltage characteristics as measured at NREL for the best CIGSS cell with a MOCVD ZnO buffer layer to date.
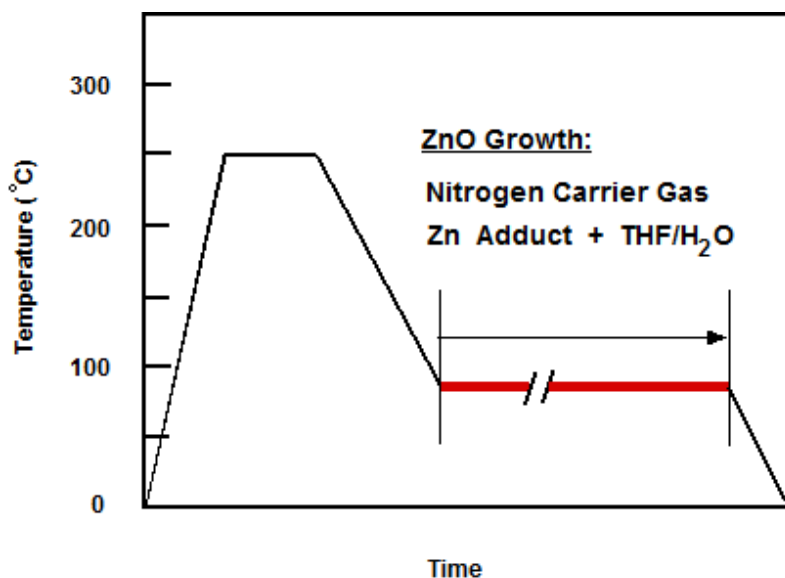


**Figure 2.   Temperature profile for MOCVD growth of i-ZnO buffer layers.**

The cell described by Figure 3 involved a team effort.   After growing the ZnO buffer layer,  the TCO was deposited by SSI and collector grids deposited by IEC. Since that time, WSU has acquired a RF sputtering system.   Now, after MOCVD growth of buffer layers, all other layers are deposited at WSU, namely, the TCO, collector grids and $MgF_2$ AR coating.

As noted, we have found that the use of KCN has proven important for achieving reasonable cell efficiencies. Thus, studies were carried out to understand the effects of the KCN surface treatment.  Surfaces of etched and unetched CIGSS were examined with XPS and Raman spectroscopy.  These measurements were conducted at the Pacific Northwest National Laboratory (PNNL) through a users agreement.  Results for XPS studies are given in Figures
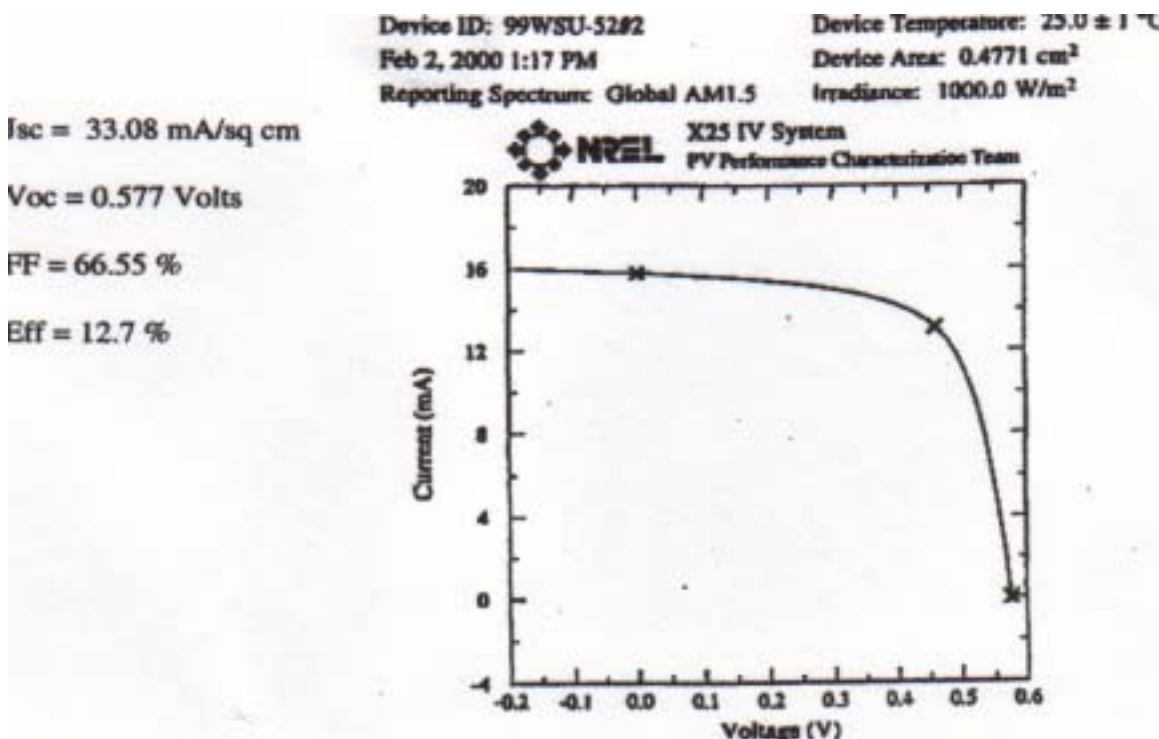
**Figure 3.** **Illuminated I-V characteristics measured by NREL for a CIGSS cell with a WSU MOCVD ZnO buffer layer. Cell area = 0.477 sq.cm. Jsc=33.08 mA/sq cm, Voc=0.577 Volts, FF=66.55% and Eff=12.7%**

4 and 5. Intensity of photoelectron emission is plotted versus binding energy for the surface of etched and unetched sample surfaces in Figure 4. Photoelectron emission is observed for the unetched sample corresponding to Se apparently in its normal site, and also due to Se bonded to oxygen in the form of $SeO_2$. In the case of the etched sample, the $SeO_2$ line is completely removed. Thus, it is clear that one effect of the KCN etching process is to remove oxygen from the surface and probably grain boundaries near the substrate surface. A XPS concentration profile of the unetched sample is shown in Figure 5. The sulfur concentration is not shown, but based on Auger concentration profiles, the selenium and sulfur surface concentrations are approximately the same. It is clear that oxygen resides at the surface, and probably along grain boundaries near the surface. XPS concentration profiles for etched samples indicate as does Figure 4 that the oxygen is essentially removed by KCN.

6
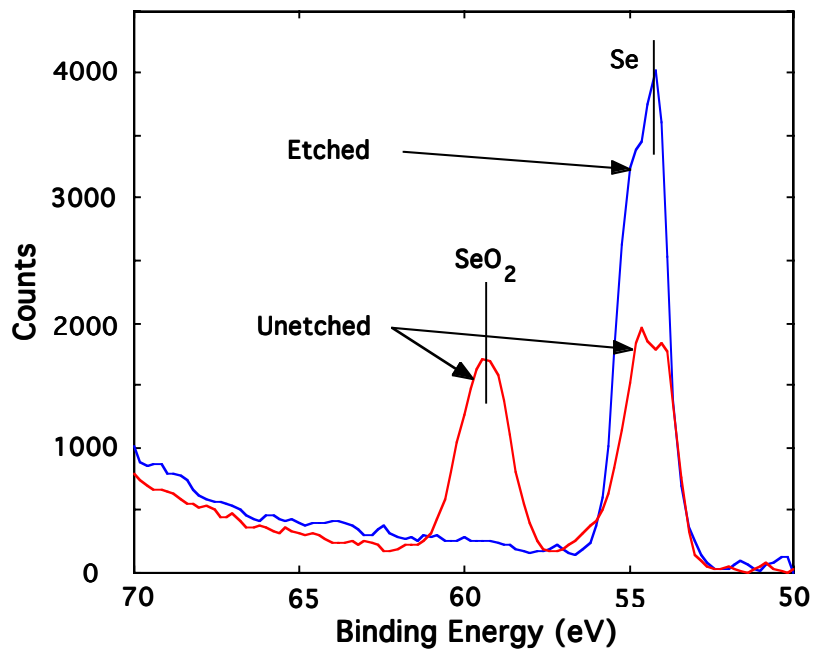
**Figure 4.** XPS spectra for two CIGSS substrates, one etched with KCN and one not etched.
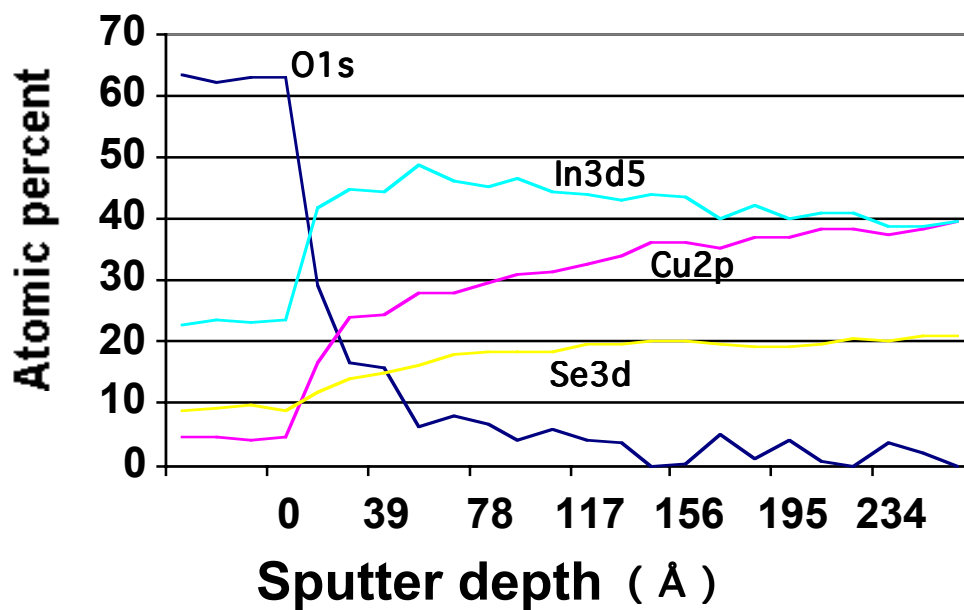


**Figure 5.** XPS depth concentration profiles for an unetched CIGSS surface.

Oxygen attached to Se at the surface would lead to Se vacancies at the surface, which constitute donors. Se vacancies should not be a problem at the

interface between CIGSS and the buffer layer since the high donor density would tend to invert the CIGSS surface. However, inverted grain boundaries near this interface would lead to excess recombination and current losses. After KCN removes the oxygen thereby allowing Se atoms to occupy the proper sites, current losses may be reduced. These effects constitute a tentative model for the beneficial effects of KCN.

Raman spectroscopic studies were also carried out on unetched and etched CIGSS material in an effort to understand the effects of the KCN etch. These studies were motivated by results obtained previously with SSI's CIS material (non-sulfur containing material). In particular, we found that KCN removed Cu-Se precipitates in the case of CIS absorbers. Plots of the Raman shift versus wavenumber for unetched CIS material exhibited lines corresponding to Cu-Se precipitates, while plots for etched CIS samples exhibited only a line corresponding to CIS. Results for Raman spectroscopic measurements on CIGSS material are given in Figure 6. Plots of the Raman shift versus wavenumber are essentially identical for the unetched and etched CIGSS samples. Thus, it appears that the SSI CIGSS material has a negligible amount of Cu-Se or Cu-S precipitates. Whereas only one line at 173 cm$^{-1}$ was observed in the case of CIS, we observed two distinct lines for CIGSS. The additional line appears to be a result of sulfur atoms be added to the unit cell of the CIGSS relative to CIS. These studies were carried out in an effort to understand the apparent need for the KCN etch when processing the SSI material. It should be noted that it is common for weeks or months to pass between the time WSU receives the SSI plates and when cells are processed. Clearly, there is ample time for surface oxidation to occur. These results may have relevance to other group's cell processing as well, however. CIS and CIS-alloys are all rather reactive, and thus one would expect surface oxidation to occur. Most cell processing involves CBD
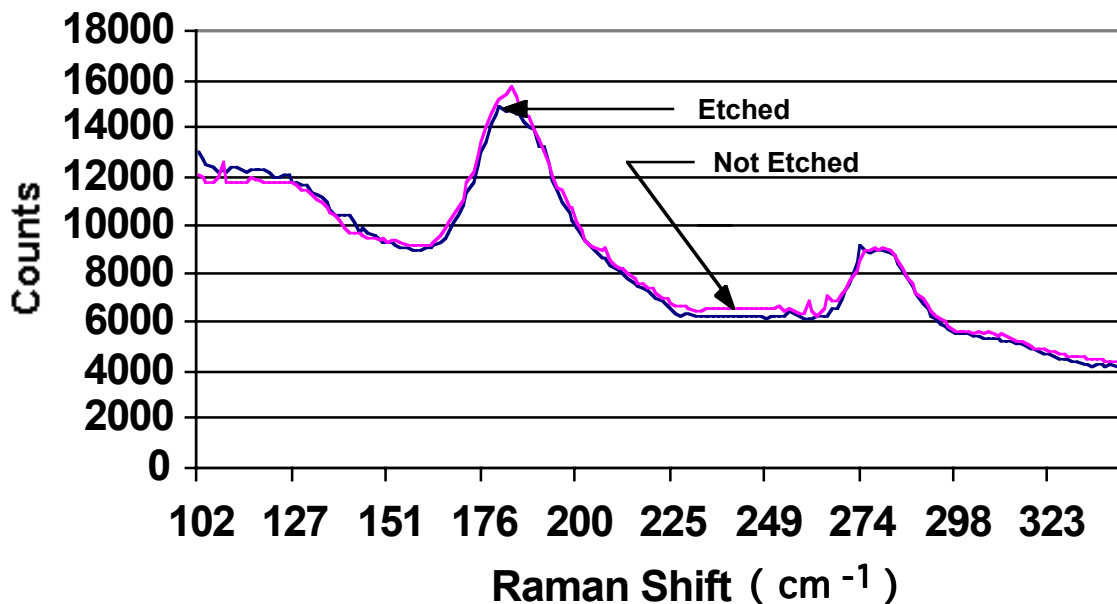
**Figure 6.** **Raman shift for KCN etched and unetched CIGSS samples.**

growth of CdS buffer layers. As determined by Ramanathan at NREL, the Cd solution reacts with a CIS surface prior to growth of CdS. We recently investigated the effect of a Cd bath solution on a SSI CIGSS surface. Figure 7 shows XPS spectra for three samples: an as-received CIGSS substrate; a CIGSS sample that has been rinsed with DI water; and a sample that has been exposed to a cadmium bath solution. After exposure to the Cd bath solution, the $SeO_2$ line is essentially removed, and the Se line is reduced as well. In addition, we find that the Cd concentration near the surface is quite significant. Both the Cd and the apparent Se vacancies can act as donors to invert the surface. The key point to be made , however, is that the usual process used by most groups probably leads to removal of the oxygen at the sample surface.
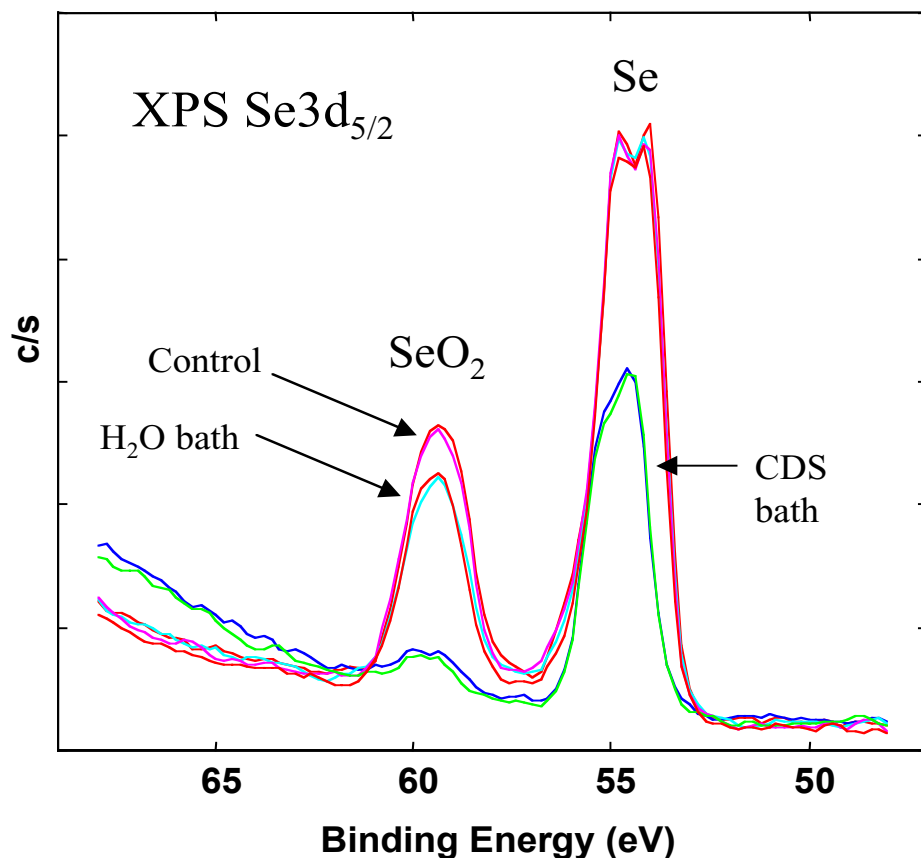
**Figure 7.** **XPS spectra for three samples: an as-received CIGSS substrate; a CIGSS sample that has been rinsed with DI water; and a sample that has been exposed to a cadmium bath solution.**

### 2.2 Characterization Of MOCVD ZnO Buffer Layers

Initially, two growth processes for ZnO buffer layers were investigated, namely, one-step and two-step methods.  The two-step process has led to efficient cells, whereas the one-step process gave only poor results.  By two-step, we refer to a process as described in Figure 2, as well as a process during which growth occurs at the 250°C stage. Buffer layers grown with these approaches have been characterized with spectroscopic ellipsometry in a collaborative effort with Dr. Gregory Exarhos of PNNL.  These studies indicate that the two-step films exhibit very abrupt band edges as expected for ZnO, whereas one-step films have rather soft band edges.   Figure 8 gives a plot of $(\alpha h\nu)^2$ vs $h\nu$ for the two types of films as determined from the extinction coefficient versus photon energy.  XRD studies indicate both types of films are crystalline, but have slightly

different spectra. Both films exhibit (100) and (002) reflections, with the one-step film showing a fairly strong (100) orientation, and with the two-step film not as well oriented. The most striking result from characterization studies of these two types of buffer layers is the difference in band edges. This effect would appear to be strongly related to the film properties that cause such differences in cell performance. The two-step process involves heating the sample to 250°C (with or without growth of a nucleation layer) before growing most of the film at 100°C. Our studies indicate that the 'high' temperature step is needed in order to grow a film that exhibits an abrupt band edge. Thus, we hypothesize the 250°C step provides thermal cleaning of the sample surface which reduces the amount of incorporated defects and impurities in the ZnO buffer layer and results in a low defect density at the ZnO-CIS interface. It is clear that cells fabricated with a one-step buffer layer are characterized by large recombination current losses. Thus, since the one-step films are crystalline, but exhibit a 'soft' band edge suggesting a high density of interband states, and result in poor cell performance when utilized as a buffer layer, we conclude that the growth process of ZnO films grown on CIS without the thermal cleaning step are affected by impurities on the CIS surface. It appears that ZnO buffer layers grown with the one-step process lead to ZnO-CIS interfaces characterized by high recombination and low cell performance.

## 2.3    Effect Of Buffer Layers On Device Performance

The effect of buffer layers on device performance is still not totally understood. Furthermore, we can not simply think of two categories of devices, those with a buffer layer and those without a buffer layer. In particular, one must recognize that CdS appears to be a very special buffer layer. Our
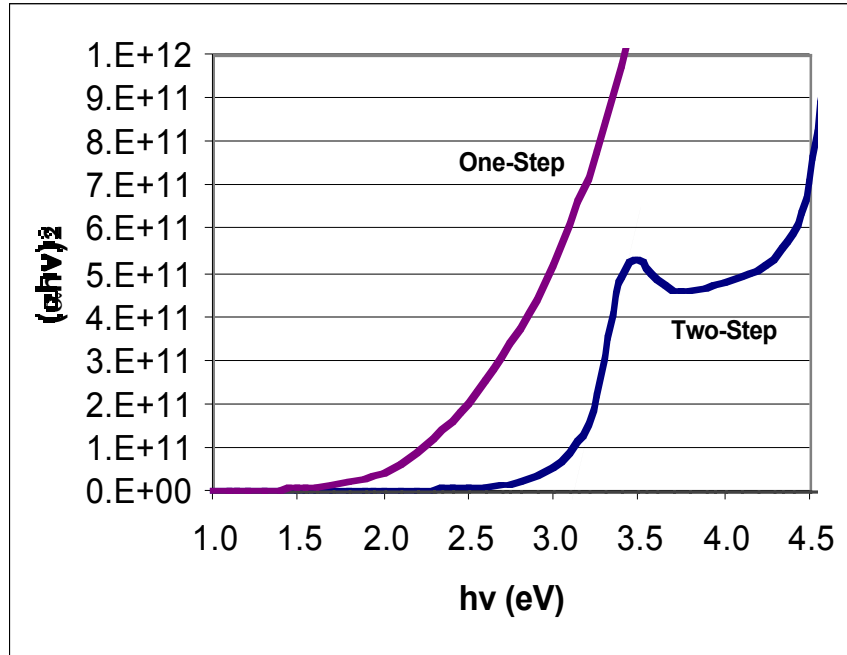
**Figure 8.** $(\alpha h\nu)^2$ **vs** $h\nu$ **for MOCVD films grown with one-step and two-step processes.**

Participation in the Transient Team studies was beneficial, in general, but it particularly brought in focus for us the clear distinction between 'direct zinc oxide ' cells and those with CdS or MOCVD ZnO buffer layers. The proposed program would include studies concerned with understanding the effect of buffer layers on cell performance. Part of the proposed effort would be to determine current loss mechanisms in direct ZnO cells. A direct ZnO cell will be defined as one formed by depositing a conductive n-ZnO layer directly onto a CIS or CIS-alloy absorber. The TCO could be deposited either by MOCVD (as with SSI) or by sputtering. We have carried out some studies that are relevant to this problem and that would form the starting point for further investigation. Although buffer layers probably serve more than one purpose, it would seem that one strong possibility is that they act as a diffusion barrier. In particular, they might inhibit diffusion of Zn or dopant atoms from the TCO into the absorber. As implied above, the buffer layer may serve another purpose such as possibly cause inversion as one might hypothesize in the case of CdS. However, the issue of a possible diffusion barrier should be addressed.

We have investigated current-voltage characteristics of direct n-ZnO/CIGSS cells and n-ZnO/CdS/CIGSS in an effort to begin to address this issue of the effect of buffer layers on cell performance. These cell structures were provided by SSI in the form of 10 cm x 10 cm plates. After breaking the plates into 2 cm x 2 cm substrates, Ag collector grids were deposited onto the substrates and cells were characterized. Typical efficiencies for the Direct n-ZnO/CIGSS cells and n-ZnO/CdS/CIGSS cells were 7 to 8 % and 12 to 14 %, respectively. Current-voltage characteristics near the maximum power point were analyzed to determine J-V parameters for the current loss component. Typical $J_0$ and A-factors are given in Table 2. Although only limited studies have been conducted, results for the direct ZnO cells suggest that the current loss mechanism may be due to multiple step tunneling since the A-factor is greater than two. This conclusion is also based on results of simulation studies carried out with PC-1D. In particular, as discussed below, studies carried out to date for CIS based cells indicate that current loss mechanisms due to Shockley-Read-Hall (SRH) recombination within the depletion region will only lead to A-factors in the 1.3 to 1.7 range. Temperature dependent studies will allow further sorting of current loss mechanisms. It is our intention to combine these studies with physical characterization studies, such as depth concentration profiles, in an effort to understand the role of buffer layers.

Although other researchers have used other programs, we have found that PC-1D is particularly useful for simulation studies. To support investigations of current-loss mechanisms in CIS cells, we are carrying out a study similar to that originally done by Sah, Noyce and Shockley for silicon devices. After selecting a model for a CIS cell current-voltage characteristics are

**Table 2 -- Typical Current Loss Parameters**

| | $J_o$ ( A/cm$^2$) | A-Factor |
|---|---|---|
| Direct n-ZnO/CIGSS Cell | $5 \times 10^{-6}$ | 2.4 |
| n-ZnO/CdS/CIGSS Cell | $2 \times 10^{-8}$ | 1.6 |

calculated. The current-voltage characteristics are then fit in the vicinity of maximum power to determine $J_0$ and A-factors that characterize the current loss component. Calculations were carried out for CIS assuming trap levels (Et) ranging from midgap ( Ei ) to the conduction band edge (or valence band edge). Preliminary results of these studies are given in Table 3. Further adjustment of parameters is needed in order to obtain values $J_0$ and A-factors as determined for cells with CdS buffer layers. But it does appear that the current loss mechanisms in cells with CdS buffer layers can be interpreted as being due to SRH recombination within the depletion region, while another mechanism must be assumed for direct ZnO cells.

**Table 3 -- Results From Analysis Of Current-Voltage Characteristics Calculated By PC-1D**

| Et - Ei | $J_o$ ( A/cm$^2$) | A-Factor |
|---|---|---|
| 0.0 | $3 \times 10^{-6}$ | 1.7 |
| 0.2 | $2 \times 10^{-6}$ | 1.6 |
| 0.4 | $1.4 \times 10^{-8}$ | 1.4 |

# 3.   CIGSS CELLS WITH CBD ZnS BUFFER LAYERS

In an effort to develop suitable alternative buffer layers for CIS-based solar cells, several groups have investigated Zn and In compounds grown by chemical bath deposition (CBD).  For example, studies have been reported for $In(S,OH)_x$, $In(OH)_2$, ZnO, ZnS, $Zn(O,S,OH)_x$, $SnO_2$ and ZnSe.  Efficiencies of 15.7% [1] and 16.9% [2] were obtained for CIGS absorbers and with chemically deposited $In_x (OH,S)_y$ and ZnS buffer layers, respectively.  This paper concerns investigations of cells fabricated from CIGSS based absorbers supplied by Siemens Solar Industries (SSI), and ZnS buffer layers grown by CBD. Details of the CBD process are discussed, and results for completed solar cells are presented. The best cell obtained to date yielded an active area ($0.42$ $cm^2$) efficiency of 13.3%.

## 3.1    CIGSS Substrate and Surface Preparation

These studies were based on SSI material CIGSS (also referred to as Graded absorber). This material has sulfur incorporated in the surface region such that the surface concentration is approximately CuInSeS and Ga concentrated near the back contact with Mo [3]. CIGSS substrates used for cell fabrication consisted of CIGSS absorber layers on Mo-coated glass.  Substrates were typically 2 cm x 2 cm in size.  Prior to CBD growth of ZnS buffer layers, substrates were subjected to a cleaning process consisting of rinses in 1,1,1 trichloro-ethane, acetone, methanol and distilled water followed by an etching  step with 10% KCN solution.   In previous studies XPS surface analyses determined that KCN removes oxygen from the surface and probably grain boundaries near the substrate surface [4].

## 3.2    ZnS Buffer Layer Growth and Characterization

Reagents used for these studies are Zinc Sulfate Hepta-hydrate ($ZnSO_4$, $7H_2O$), Ammonium Sulfate [$(NH_4)_2SO_4$], Thiourea [$SC(NH_2)_2$], Ammonium Hydroxide and Hydrazine Hydrate. Complexing agents play an important role in the growth process. The effects on solar cell performance of reagent composition, deposition time, bath temperature and bath pH have been investigated.  The approach to chemical bath deposition involves mixing the desired masses of $ZnSO_4$, $7H_2O$ and $(NH_4)_2SO_4$ into the

beaker containing stirred deionized water at about $80^0$C, with cleaned substrates held in place with a rotating Teflon holder. When the mixture is completely dissolved, the required mass of complexing agents are added to the solution. One objective of the study is to identify optimum growth conditions for CBD ZnS buffer layers to maximize efficiency. The best cell efficiency obtained to date is 13.3% (active area).

### 3.3    Cell Completion and Device Analysis

After growth of ZnS buffer layers, cells were completed by depositing n-ZnO TCO layers followed by deposition of Ag grids. TCOs were deposited by MOCVD at SSI. Ag grids were deposited such that each 2 cm x 2 cm substrate contained three individual cells with total areas of approximately 0.45 $cm^2$. Numerous cells have exhibited efficiencies greater 10 %. Some of these results are tabulated in Table 1. One of the cells was sent to NREL for I-V characterization. The quantum efficiency and illuminated I-V characteristics as measured by NREL are given in Figures 1 and 2, respectively. The spectral quantum efficiency measurement shows a significant gain below 540 nm (the absorption edge of CdS) due to higher band gap of ZnS. Current voltage analysis are being conducted with the objective of comparing current loss mechanisms in these cells to CIGSS cells based on CdS buffer layers. Finally, efforts are concentrating on processing that will lead to improved fill factors.

**Table 4** -- **Cell Results With ZnS Buffer Layers**
**(Based on active cell area of 0.42 $cm^2$)**

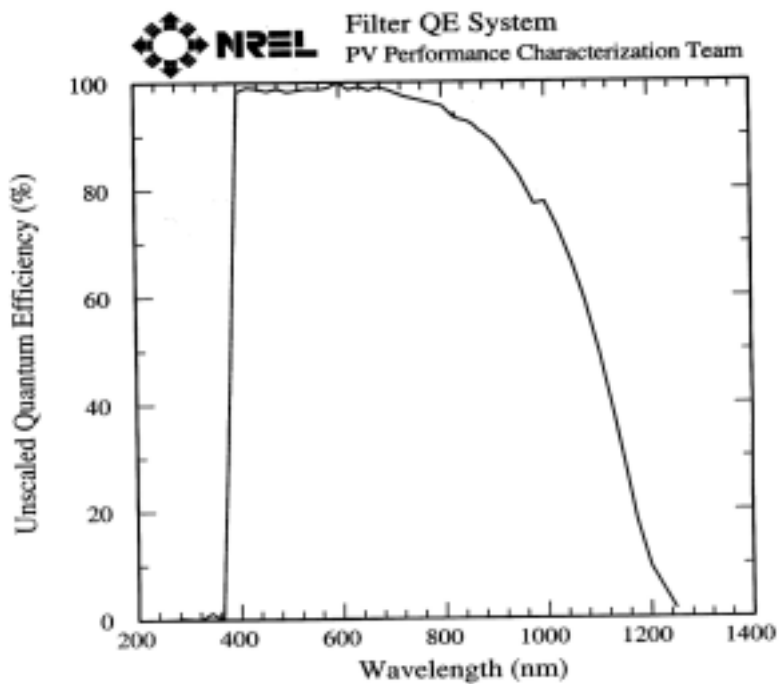| Sample | $E_{ff}$(%) | FF(%) | $V_{oc}$ ( mV) | $J_{sc}$(mA/cm$^2$) |
|---|---|---|---|---|
| 01-30 | 11.0 | 56.0 | 535 | 36.82 |
| 01-33 | 11.7 | 57.2 | 552 | 37.07 |
| 01-34 | 10.6 | 52.8 | 549 | 36.56 |
| 01-35 | 10.7 | 54.0 | 532 | 37.33 |
| 01-36 | 11.7 | 57.1 | 540 | 38.00 |
| 01-37A | 13.3 | 61.4 | 552 | 39.35 |
| 01-37B | 12.1 | 57.7 | 542 | 38.58 |

16

**Figure 9. Quantum efficiency measured by NREL for cell WSU-01-37A.**



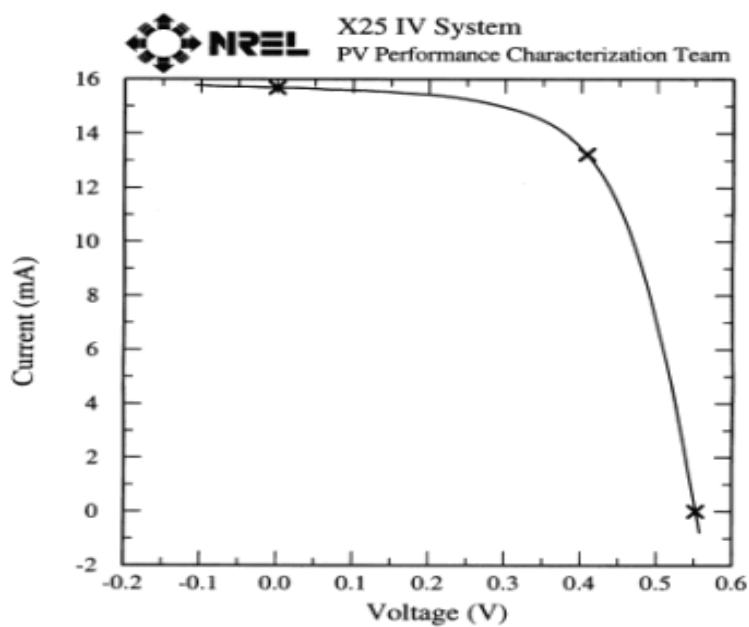**Figure 10. Illuminated I-V characteristics measured by NREL for cell WSU-01-37A: Jsc = 35.8 mA/sq cm, Voc = 0.552 , FF = 0.604 and Total Area Eff = 12.3 %.**

## 4.  EFFECT OF BUFFER LAYERS ON DEVICE PERFORMANCE

In an effort to understand the effects of buffer layers on CIS-based solar cells,  two types of devices are being investigated, namely, direct ZnO cells defined as a structure with conductive n-ZnO deposited directly onto a CIGSS substrate, and cells with effective buffer layers.  In particular, CdS grown by CBD and highly resistive ZnO(i-ZnO) grown by MOCVD were utilized as buffer layers.  Although buffer layers probably serve more than one purpose, it would seem that one strong possibility is that they act as barriers to diffusion of impurities from TCO layers into absorbers.  Clearly, buffer layers may serve other purposes such as to provide interface passivation or to establish an inverted region in the absorber.  The focus of this paper is to examine the possibility that buffer layers serve as barriers to diffusion of undesirable impurities into CIS-based absorbers.  Although the studies have utilized only CIGSS absorbers made by Siemens Solar, Industries (SSI), general conclusions about the role of buffer layers in CIS-based cells are proposed.

### 4.1     Cell Fabrication and Performance

Three cell structures were investigated.  Layered structures appropriate for direct n-ZnO/CIGSS and n-ZnO/CdS/CIGSS cells were provided by Siemens Solar Industries (SSI) in the form of 10 cm x 10 cm plates.  After dicing the plates into 2 cm x 2 cm substrates, Ag collector grids were deposited onto the substrates, cells defined and characterized.  SSI also provided 10 cm x 10 cm plates of CIGSS on Mo coated glass.  These plates were diced into 2 cm x 2 cm substrates and used to fabricate cells with i-ZnO buffer layers.  Measured efficiencies for the three types of cells are typically 7 to 9 % for direct cells, 11 to 14 % for cells with CBD CdS and MOCVD i-ZnO buffer layers.   The best results for cell performance obtained to date for a MOCVD ZnO buffer layer are described in Figure 3.

### 4.2     Physical Characterization

SIMS depth concentration profiles of the CIGSS absorber regions have been carried out for direct cells and devices with CdS buffer layers.  Profiles have not yet been carried out on cells

with i-ZnO buffer layers.  SSI TCO layers (boron doped ZnO) and CdS layers were removed using a 15 second etch in 50% (by volume) HCl in water solution.  It was determined that this procedure removes the SSI TCO layer (typically 1.7 μm) and CdS buffer layer.  The required time of etching was determined by creating a step height with photoresist and then measuring the step height with a Zygo interferometer.  A similar method was used to determine that the HCl solution only removes CIGSS at a rate of 0.25 A/s.  Thus, the process used to remove the TCO and CdS layers only removes a few angstroms of the CIGSS absorber.

Depth concentration profiles for a given sample were acquired after various amounts of CIGSS was removed with a bromine etchant.   This approach results in smoother surfaces which improves one's ability to interpret data.  The bromine etching solution consisted of a mixture of 0.02 mol/l $Br_2$ and 0.1 mol/l KBr.  Again using a Zygo interferometer, we determined that this etchant removed CIGSS at rate of 2.4 A/s.  Following a bromine etch all samples were cleaned with hot trichlorethlene, acetone, methyl alcohol and di-ionized water.  Zygo images clearly established that substantial surface smoothing occurs with the bromine etching process.

TOF-SIMS was chosen for depth profiling because of its sensitivity to impurities that might diffuse into CIGSS absorbers from TCO layers during cell fabrication.  Nominal sensitivity of the TOF-SIMS is in the parts per billion range.  The data reported here were obtained by averaging two areas on the CIGS surfaces. Residual hydrocarbon was removed with a light sputter, 30 seconds at 600 pA $Ga^+$ over a 200 x 200um region.  Based on calibration with $SiO_2$ this procedure should remove 3 angstroms.

SIMS data taken at various depths for direct cells and CdS buffered cells are shown in Figure 11.   The data for direct cells show a significant concentration of aluminum.  On the other hand,  no impurity concentration was detected in the CdS buffered cells, except for cadmium (not shown).  Further studies need to be carried out, but we tentatively conclude that Cd appears to diffuse a few hundred angstroms into CIGSS.   Since SSI currently dopes their TCO with boron, the aluminum impurity concentration may seem puzzling.  However, it is quite possible aluminum was utilized in the past.  The direct cell structures used in these studies were grown by SSI in 1998.  We intend to have results for current technology structures in time for the meeting.  The

key point to be made, however, is impurity diffusion into CIGS absorbers is evident for cells without CdS buffer layers.
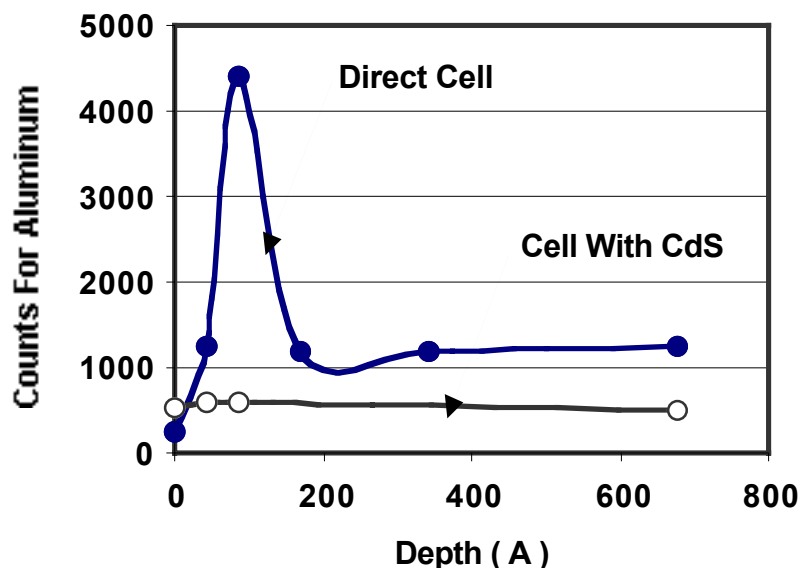


**Figure 11.   SIMS-TOF profiles for aluminum in direct and CdS buffered CIGSS Cells.**

### 4.3      Current Loss Mechanisms

Dark current-voltage characteristics for the two types of cells were analyzed to determine J-V parameters for the current loss components.  To date, only dark characteristics have been investigated.  Illuminated characteristics and temperature dependent analyses are in progress. Typical $J_o$ and A-factors for dark characteristics are as follows: Direct cells, $J_o$ = 5E-6 A/cm$^2$, A>2; CdS buffered cell, $J_o$ = 2E-8 A/cm$^2$, A = 1.6.  Results for n-ZnO/i-ZnO/CIGSS cells are similar to those for CdS buffered cells.   Although only limited studies have been conducted, results for the direct ZnO cells suggest that the dominant current loss mechanism in these devices is not explained by SRH recombination.   These cells are usually characterized by an A-factor significantly greater than 2.0.  Simulation studies conducted with the aid of PC-1D for CIS-based cells indicate that SRH recombination due to traps in the depletion region should lead to A-factors

in the range of 1.3 to 1.7, as the trap level is varied from the band edge to the midgap point. A-factors greater than 2.0 can be due to multiple step tunneling, or tunneling mechanisms combined with recombination processes. Such an explanation would be consistent with the higher impurity concentration level in direct cells. On the other hand, PC-1D studies suggest that CIGSS cells with CdS buffer layers are characterized by current loss mechanisms due to SRH recombination via interband states. Figure 12 describes results obtained from PC-1D simulations. Current-voltage characteristics are calculated using PC-1D, and then effective values for $J_o$ and A are determined for the simulated J-V characteristics in the voltage range of 0.3 to 0.6 Volts. The approach to this study is similar to that used by Sah, Noyce and Shockley for silicon devices. To date, a single trap level has not been identified that simultaneously gives values for Jo and A that agrees with experimental results.
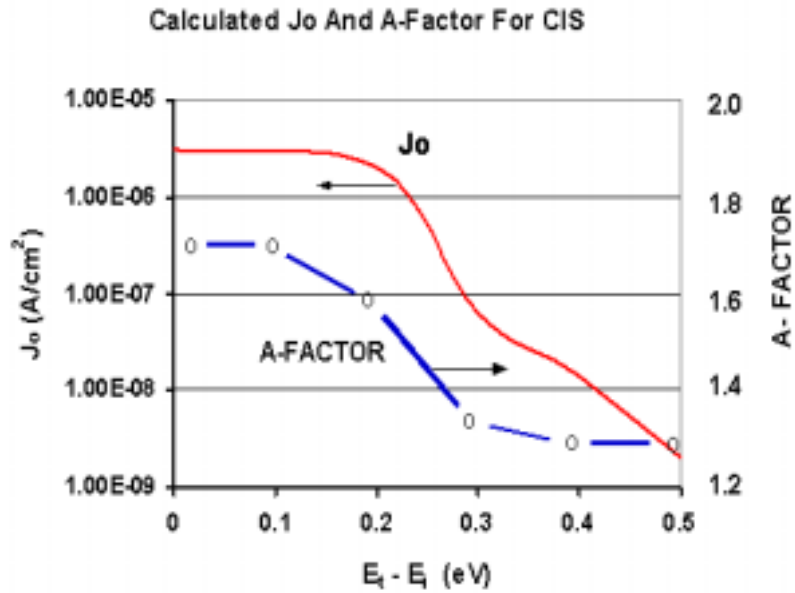


**Figure 12.** **I-V parameters determined for simulated current-voltage characteristics determined with PC-1D.**

# 5.  CONCLUSIONS

Investigations of CIGSS cells based on ZnO and ZnS buffer layers have resulted in cells with total area efficiencies on the order of 13%.  ZnO buffer layers were grown by MOCVD and ZnS layers were deposited by chemical bath deposition.  The effect of the WSU surface preparation was studied with the help of XPS analyses.  The initial step in the WSU cell fabrication process involves cleaning of the CIGSS surface followed by an etching step with KCN.  Studies were carried out to characterize the effect of the KCN step.  Using XPS surface analyses as well as XPS depth concentration profiles, it was determined that the KCN etching process removes oxygen from the surface that had reacted with the CIGSS surface to form $SeO_2$.  Removal of oxygen from the CIGS surface allows one to fabricate efficient CIGSS cells.   It appears that removal of oxygen allows Se to re-occupy normal Se sites, which may in turn prevent large shunting currents.  MOCVD ZnO buffer layers lead to efficient cells only if a two step growth process is utilized as opposed to a simpler one step approach.  Spectroscopic ellipsometry was utilized to determine that a two step MOCVD growth process leads to ZnO layers with a well defined conduction band edge whereas a simpler one step process results in more amorphous-like films.  In an effort to understand the positive effects of buffer layers in CIS solar cells, I-V analyses have been combined with modeling studies using PC-1D.  Current loss mechanisms were determined for Direct n-ZnO/CIGSS and cells with CdS buffer layers.  Direct cells have relatively large current losses appearing to be due to multiple step tunneling, whereas current loss mechanisms in devices with CdS buffer layers appear to be characterized by Shockley-Read-Hall  recombination.  Based on the I-V analyses and results of SIMS depth concentration profiles,  it appears that one of the primary benefits of buffer layers is to provide a barrier to impurity diffusion from the TCO.

**Publications:**

1. L.C. Olsen, et al., "Alternative Buffer Layers For CuIn(Ga)Se$_2$ Solar Cells, 15th NCPV Photovoltaics Program Review, September 1998, AIP Conf Proc 462, pp 164, Mowafak Al-Jassim, John P. Thornton and James M. Gee, Editors.

2. L.C. Olsen, et al., "Characterization of MOCVD ZnO Buffer Layers for CIS Solar Cells,"  Presented at the American Vacuum Society 46th International Symposium, October 25-29, 1999, Seattle, WA.

3. L.C. Olsen et al., Effects Of Buffer Layers On CIGSS Cell Performance, 16$^{th}$ NCPV Photovoltaics Program Review, March 2000.

4. L.C. Olsen, et al.,   CIGSS Solar Cells Based On CVD  ZnO Buffer Layers,   28$^{th}$ IEEE PVSC,  Anchorage, AK,  17-22 September 2000.

| REPORT DOCUMENTATION PAGE | *Form Approved* *OMB NO. 0704-0188* |
|---|---|

Public reporting burden for this collection of information is estimated to average 1 hour per response, including the time for reviewing instructions, searching existing data sources, gathering and maintaining the data needed, and completing and reviewing the collection of information. Send comments regarding this burden estimate or any other aspect of this collection of information, including suggestions for reducing this burden, to Washington Headquarters Services, Directorate for Information Operations and Reports, 1215 Jefferson Davis Highway, Suite 1204, Arlington, VA 22202-4302, and to the Office of Management and Budget, Paperwork Reduction Project (0704-0188), Washington, DC 20503.

| 1. AGENCY USE ONLY (Leave blank) | 2. REPORT DATE<br>January 2003 | 3. REPORT TYPE AND DATES COVERED<br>Final Report<br>1 January 1998 – 31 August 2001 |
|---|---|---|

| 4. TITLE AND SUBTITLE<br>Alternative Heterojunction Partners for CIS-Based Solar Cells: Final Report,<br>1 January 1998 – 31 August 2001 | 5. FUNDING NUMBERS<br>PVP3.5001<br>XAF-8-17619-06 |
|---|---|

6. AUTHOR(S)
L. C. Olsen

| 7. PERFORMING ORGANIZATION NAME(S) AND ADDRESS(ES)<br>Electronic Materials Laboratory<br>Washington State University at Tri-Cities<br>Richland, Washington | 8. PERFORMING ORGANIZATION REPORT NUMBER |
|---|---|

| 9. SPONSORING/MONITORING AGENCY NAME(S) AND ADDRESS(ES)<br>National Renewable Energy Laboratory<br>1617 Cole Blvd.<br>Golden, CO 80401-3393 | 10. SPONSORING/MONITORING AGENCY REPORT NUMBER<br><br>NREL/SR-520-33362 |
|---|---|

11. SUPPLEMENTARY NOTES
NREL Technical Monitor: B. von Roedern

| 12a. DISTRIBUTION/AVAILABILITY STATEMENT<br>National Technical Information Service<br>U.S. Department of Commerce<br>5285 Port Royal Road<br>Springfield, VA 22161 | 12b. DISTRIBUTION CODE |
|---|---|

13. ABSTRACT *(Maximum 200 words):* This report summaries work carried out in three areas: CIGSS cells based on ZnO buffer layers, cells with ZnS buffer layers, and general studies of the effects of buffer layers on device performance. These investigations were conducted mainly with CIGSS substrates provided by Siemens Solar Industries. ZnO buffer layers were grown by MOCVD and ZnS layers were deposited by chemical-bath deposition. Active-area efficiencies of 13.4% and 12.8% were achieved for cells based on ZnO and ZnS buffer layers, respectively. The initial step in the Washington State University cell fabrication process involves cleaning of the CIGSS surface, followed by an etching step with KCN. Studies were carried out to characterize the effect of the KCN step. Using XPS surface analyses, as well as XPS depth concentration profiles, it was determined that the KCN etching process removes oxygen that had reacted with the CIGSS surface to form $SeO_2$. Removal of oxygen from the CIGSS surface allows one to fabricate efficient CIGSS cells. Spectroscopic ellipsometry was used to determine that a two-step MOCVD growth process leads to ZnO layers with a well-defined electron-band structure, whereas a simpler one-step process results in more amorphous-like films. In an effort to understand the positive effects of buffer layers in CIS solar cells, I-V analyses have been combined with modeling studies using PC-1D. Although buffer layers may provide passivation at the surface, and possibly inversion in some cases, we conclude that it is also likely that buffer layers provide barriers to impurity diffusion resulting from deposition of TCO layers.

| 14. SUBJECT TERMS: PV; spectroscopic ellipsometry; electron-band structure; RF sputtering; heterojunction; CIS; buffer-layer; device performance; XPS; modeling; TCO | 15. NUMBER OF PAGES |
|---|---|
| | 16. PRICE CODE |

| 17. SECURITY CLASSIFICATION OF REPORT<br>Unclassified | 18. SECURITY CLASSIFICATION OF THIS PAGE<br>Unclassified | 19. SECURITY CLASSIFICATION OF ABSTRACT<br>Unclassified | 20. LIMITATION OF ABSTRACT<br>UL |
|---|---|---|---|